



## Development of bimetallic nanoparticles and their electro catalytic activity

Chetna M Zaveri

Department of Chemistry, Kirti Doongursee College, Dadar, Mumbai, Maharashtra, India

### Abstract

In the present study methanol permeability was carried out using a diaphragm diffusion cell, consisting of two reservoirs separated by an electrolyte membrane with a dense layer of composite membranes to reproduce a phenomenon of methanol crossover in DMFC system. The results revealed that it is possible to synthesize Pt-Ni, Pt- Pu AND Pt- Mo nanoparticles of ~3–8 nm in diameter at temperatures of about 30°C. The catalytic properties of the bimetallic PtBi and PtPb nanoparticles were studied and compared with monometallic platinum nanoparticles. Firstly, the electrochemical oxidation of formic acid to carbon monoxide was investigated, and it was found that the resistance of the PtBi and PtPb nanoparticles against the catalyst-poisoning carbon monoxide was significantly higher compared to the Pt nanoparticles. Comparing the two bimetallic nanoparticles, one sees that the PtPb NPs are significantly more active than the respective PtBi NPs.

**Keywords:** bimetallic nanoparticles, electro catalytic activity, Pt-Ni, Pt- Pu and Pt- Mo

### Introduction

Global warming and greenhouse emissions are two critical issues currently addressed by the scientists all over the world. Some greenhouse gases, such as CO<sub>2</sub>, occur naturally and are emitted to the atmosphere through natural processes and human activities. Recent research also shows that the amount of CO<sub>2</sub> produces from a small car can be reduced by as much as 72% when powered by a fuel cell running on hydrogen reformed from natural gas instead of a gasoline internal combustion engine (Perry *et al.*, 2002) [2]. In addition, the world's fossil fuel reserve is limited; hence, alternative and green energy sources are required for better future of our next generation. Hydrogen is the most attractive fuel for fuel cells. It has excellent electrochemical reactivity, provides high levels of power density, and has zero emission characteristics. Nevertheless, distribution and storage difficulties currently pose serious disadvantages to the use of pure hydrogen as the feed for fuel cells in automotive-propulsion (Kordes, 1996) [3, 5]. Metal nanoparticles possess a high catalytic efficiency and large surface-to-volume ratio. A large variety of methods including impregnation, colloidal deposition, supercritical fluid, and electrode position have been reported for the synthesis of Pt-Ru nanoparticles. The electrochemical route is an effective procedure when compared with others which are intricacy of the fabrication steps and impurity might be involved during the preparation (Hirschenhofer *et al.*, 2002) [4, 7]. Methanol Crossover is another problem in direct methanol fuel cell. In PEM fuel cells, one of the objectives of the membrane is to stop fuel and oxygen to reach the electrode on the other side and undergo non-electrochemical oxidation. Electrons are brought directly from the anode to the cathode along with methanol resulting in an internal short circuiting and consequently a loss of current (Blomen *et al.*, 2002). Besides, the cathode catalyst, which is pure platinum, is fouled by methanol oxidations intermediates similar to anode.

### Materials and Methods

The most significant part of a direct methanol fuel cell is the membrane electrode assembly (MEA). Its basic structure consists of the polymer electrolyte membrane (PEM), two catalyst layers and two diffusion layers. The polymer electrolyte membrane, which separates the anode and the cathode compartment, preferably allows for proton transport. The anodic and cathodic electrochemical reactions take place within the connected catalyst layers directly attached to the surface of the polymer electrolyte membrane (PEM). The diffusion layers on either side of the membrane electrode assembly MEA provide for good electrical contact of the catalyst layers across the whole surface.

### Experimental

#### Preparation of Nafion/SiO<sub>2</sub>/TiO<sub>2</sub> composite membranes

Nafion/SiO<sub>2</sub>/TiO<sub>2</sub> composite membranes were prepared via in situ sol gel reaction. Firstly, the Nafion 117 membrane was dried at 80°C for five hrs. Then the membrane was dipped into the methanol/water solution and kept for 1 hr. Afterwards, the sample was rubbed out with filter paper. The membrane was then immersed into various proportion of CH<sub>3</sub>OH-H<sub>2</sub>O/C<sub>2</sub>H<sub>5</sub>OH-Tetra ethoxysilane (TEOS)/Titanium isopropoxide (Ti(O-*i*-Pr)<sub>4</sub>) mixture solution for five minutes and then membranes were soaked in 0.5 M H<sub>2</sub>SO<sub>4</sub> for one hour. Finally membranes were rinsed with deionized water.

#### Methanol, oxygen permeability

Experiment to evaluate methanol permeability was carried out using a diaphragm diffusion cell, consisting of two reservoirs separated by an electrolyte membrane with a dense layer of composite membranes to reproduce a phenomenon of methanol crossover in DMFC system. The PEM is sandwiched between compartments. Initially the one compartment was filled with 50 ml of aqueous methanol

solution and other compartment with 50 ml of deionized water. The solution in each bath was stirred using magnetic stirrer during measurement to keep uniform concentration. Due to the presence of liquid water on either side of the cell, the membrane remains hydrated. Equal amount of solution in both the compartments ensures that equal hydrostatic pressure is maintained. The change in concentration of methanol in receptor compartment was measured for various composite membranes. The methanol permeability across the Nafion 117/ SiO<sub>2</sub>/ TiO<sub>2</sub> composite membrane was measured by taking 50 ml of 5%, 10% and 30% methanolic solution on one side of the membrane and 50 ml of water on other side the membrane was equilibrated. In this condition liquid sample of 50 μL were taken every 30 min. from the permeate compartment and analysis was carried out by colorimetric micro-determination method using chromotropic acid.

### Colorimetric micro-determination of methanol

10 cc of sample solution in 50 cc standard measuring flask was treated with H<sub>3</sub>PO<sub>4</sub> and KMnO<sub>4</sub> solution. The solution was kept for 10 min at room temperature with occasional swirling to ensure oxidation of methanol to formaldehyde. Sodium bisulphate is then added drop wise to reduce excess of KMnO<sub>4</sub>. Solution was cooled and kept in ice bath and 4 ml of cold conc. H<sub>2</sub>SO<sub>4</sub> and four drops of chromotropic acid

reagent were added. Flask was kept in water bath at 60° C for 15 min. The solution was diluted up to the mark with distilled water. Using distilled water as a blank, absorbance of the solution and standard were measured at 580nm.

### Preparation of precursor complexes

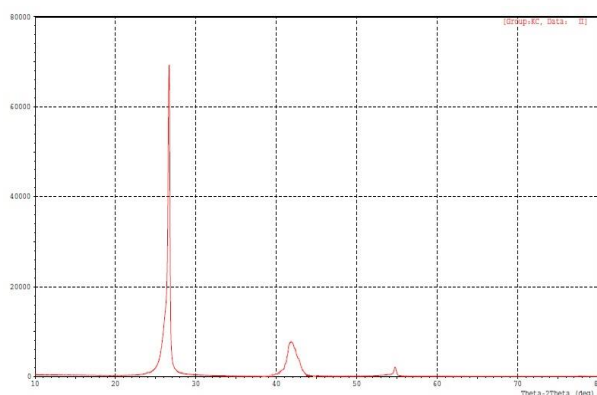
For DMFC anode catalyst, Pt-Ni/C and Pt-Mo/C metal alloy on carbon NCK-77 were prepared using molecular precursors as a source of metal.

Metal alloy loading is controlled by adjusting the relative masses of precursor compound and carbon support

### Result and Discussion

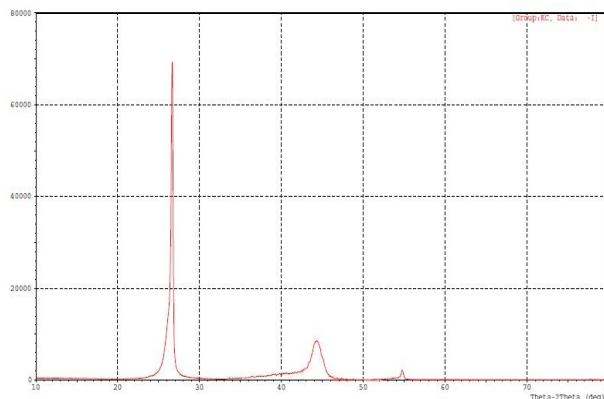
Experiment to evaluate methanol permeability was carried out using a diaphragm diffusion cell, consisting of two reservoirs separated by an electrolyte membrane with a dense layer of composite membranes to reproduce a phenomenon of methanol crossover in DMFC system. Using appropriate cell design, treating Nafion 117 with 1:1TEOS and Ti(O-i-Pr)<sub>4</sub> significant drop in methanol crossover was achieved.

Pt-Ni/C and Pt-Mo nano composites were prepared using repetitive deposition to ensure both high total metal loading and formation of well dispersed Pt-Ni and Pt-Mo alloy nano crystals. Following each cycle of precursor deposition, the precursor/C composite is heated up to 280°C. Pt/C, Ni/C



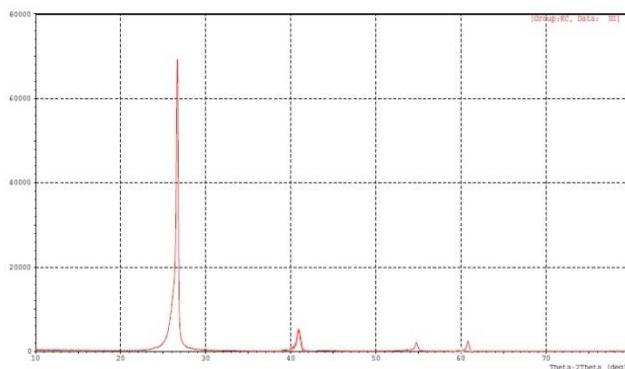
1. Pt/c

$$D = 0.94 \lambda_{K\alpha 1} / B_{2\theta} \cos \theta_B \\ = 0.9 \times 11 \times 10^{-9} / 2 \times \cos 42 \\ = 6.6 \text{ nm}$$



2. Ni/C

$$D = 0.94 \lambda_{K\alpha 1} / B_{2\theta} \cos \theta_B \\ = 0.9 \times 11 \times 10^{-9} / 3.5 \times \cos 45 \\ = 4.000 \text{ nm}$$



3. Mo/c

$$D = 0.94 \lambda_{K\alpha 1} / B_{2\theta} \cos \theta_B \\ = 0.9 \times 11 \times 10^{-9} / 2 \times \cos 41 \\ = 6.5 \text{ nm}$$

### The membrane-electrode assembly set up

The cell typically consists of graphite bipolar plates, gaskets, two electrodes and an ion conducting membrane. The bipolar plates are pressed against the electrode with gaskets for sealing and collecting current. The membrane-electrode assembly (MEA), which consists of the proton conducting membrane sandwiched between two electrodes (anode and cathode), is the heart of a PEM fuel cell. In each electrode, there is a catalyst layer and a gas-diffusion backing layer. The membrane-electrode assembly (MEA), which consists of the proton conducting membrane sandwiched between two electrodes anode and cathode. In each electrode, there is a catalyst layer and a gas-diffusion backing layer. The membrane electrode assembly having an active area of 9.0 cm<sup>2</sup> was fabricated employing a Nafion 117 membrane and two electrodes. The employed Nafion 117 membrane with a thickness of 125 μm was pre-treated in this work. The pre-treatment procedures included boiling the membrane in 5 vol.% H<sub>2</sub>O<sub>2</sub>, washing in DI water, boiling in 0.5 M H<sub>2</sub>SO<sub>4</sub> and washing in DI water for 1 h in turn. Nafion/SiO<sub>2</sub>/TiO<sub>2</sub> composite membranes were prepared via in situ sol gel reaction. Firstly, the Nafion 117 membrane was dried at 80°C for five hrs. Then the membrane was dipped into the methanol/water solution and kept for 1 hr. After wards, the sample was rubbed out with filter paper. The membrane was then immersed into various proportion of CH<sub>3</sub>OH-H<sub>2</sub>O/C<sub>2</sub>H<sub>5</sub>OH-Tetra ethoxy silane (TEOS)/Titanium isopropoxide (Ti(O-i-Pr)<sub>4</sub>) mixture solution for five minutes and then membranes were soaked in 0.5 M H<sub>2</sub>SO<sub>4</sub> for one hour. Finally membranes were rinsed with deionised water. Composite membrane was placed between the two catalytic electrodes which were supported by graphite gas diffusion layers. This catalyst layer is in good contact with the membrane, which serves as the electrolyte and the gas separator in the cell. The membrane electrode assembly was fixed between two bipolar grooved graphite plate which were designe to serve methanol and oxygen. The catalysts for the anode were loaded with Pt-Ni/C and Pt-Mo/C each metal were loaded 1g/cm<sup>2</sup>.the catalyst for cathod was loaded Pt/C. cathode Pt loading were 2.0 mg/cm<sup>2</sup>.

The methanol solution containing 50 ppm CO of several concentrations of methanol (0.5 - 3 mol/L) was served into the anode at a flow rate of 0.5 - 5 mL/min. Oxygen was served to the cathode at 150 mL/min with humidification. Figure 1 shows the cell performance at 300 K and that at 353 K for comparison. The methanol flow rate was varied from 0.5 to 05 mL/min. The performance of the DMFC system dropped at 318 K for all flow rates in comparison with 353K. The lower flow rate showed a slightly better performance. At 333 K, both the open circuit voltage and the current density at 0.4V decreased with increasing flow rate. Although a similar tendency was observed at 318 K, the dependence of the methanol flow rate on the DMFC performance was small because of the low temperature. Figure 1 shows the cell performance at 318 K at different methanol concentrations with the flow rate of 0.5 mL/min. The open circuit voltage decreased with increasing the methanol concentration to 3 mol/L, because the crossover of methanol formed a mixed potential. In case of the methanol concentration of 1.5mol/L, The current density seemed to approach a limiting value. The

study shows that in the over potential range relevant to the fuel cell anode 0.1 V- 0.5 V, the performance of Pt-Mo/C catalyst is better than the Pt-Ni/Ccatalyst at 60 °C in the lower current density range using 50 ppm CO.

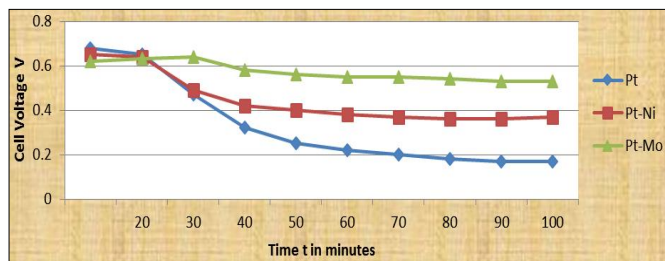


**Fig 1:** Anode feed 2M methanol 0.5 ml/min, cathode feed O<sub>2</sub> 150ml/min at 318K

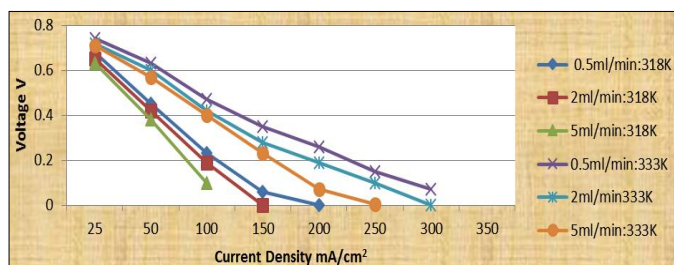


**Fig 2:** Anode catalyst- pt-/C anode feed 2M methanol.

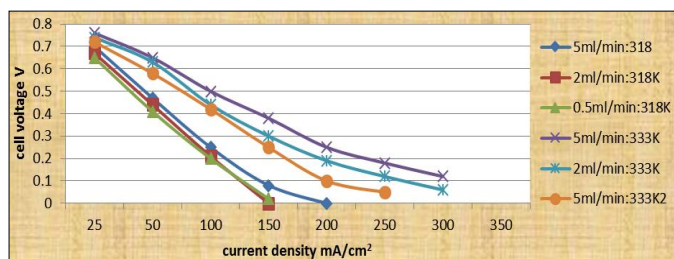


**Fig 3:** Anode catalyst- pt-Ni/C anode feed 2M methanol.

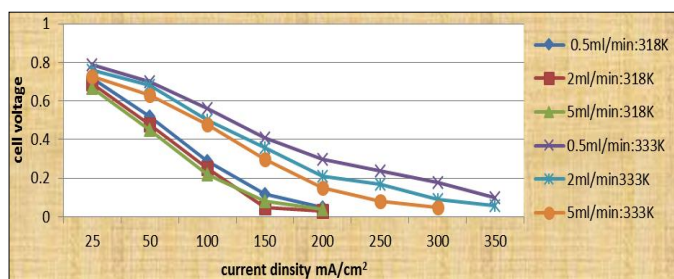


**Fig 4:** Anode catalyst- pt-Mo/C anode feed 2M methanol.

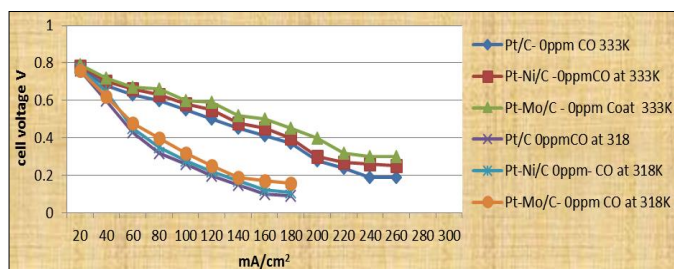


**Fig 5:** Anode flow rate 0.5 ml 1M methanol /min

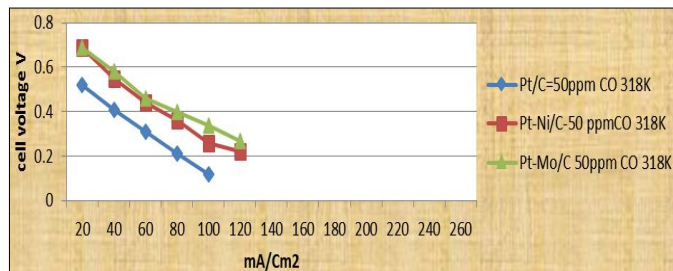


**Fig 6:** Anode flow rate 0.5 ml 1M methano with 50 ppm dissolved CO /min

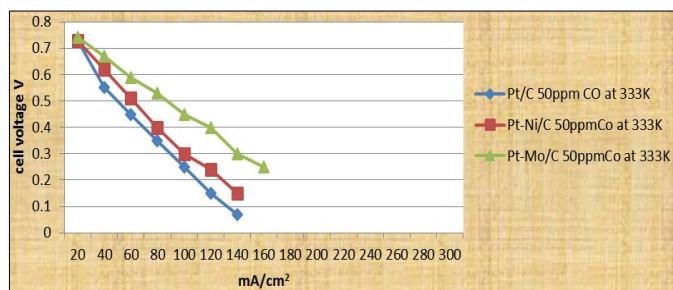


**Fig 7:** Anode flow rate 0.5 ml 1M methanol 50 ppm dissolved CO /min at 333

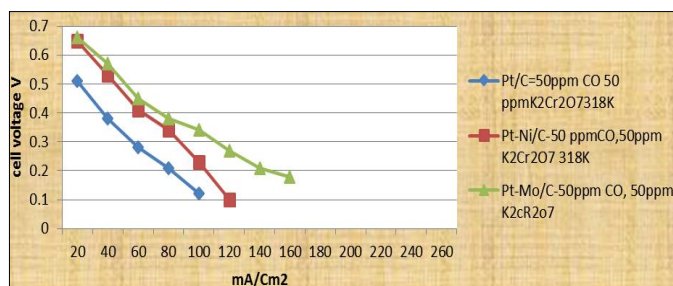


**Fig 8:** anode flow rate 0.5 ml 1M methanol with 50 ppm dissolved CO and 50 ppm K<sub>2</sub>Cr<sub>2</sub>O<sub>7</sub> /min

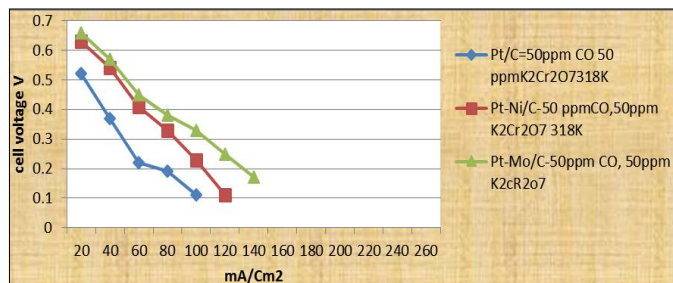


**Fig 9:** Anode flow rate 0.5 ml 1M methanol with 50 ppm dissolved CO and 50 ppm K<sub>2</sub>Cr<sub>2</sub>O<sub>4</sub> /min

XRD image 1 for Pt/C shows the partial size of 6.6nm of Pt on carbon support NCK-77. XRD. Image 2, for Ni/C shows partial size of 4nm on carbon support NCK-77. XRD image 3 for Mo/C show the partial size of 6.5 nm on the C carbon support NCK-77.

Variation of cell voltage with respect to time at constant current density shows the better performance of Pt-Mo catalyst. Fig 1 shows the maximum drop of 500mV in cell voltage when Pt/C was used as catalyst. The performance of Pt-Ni is comparatively better than Pt/c as voltage drop was

280mV. The minimum voltage drop of 80 mV was observed for Pt-Mo /C catalyst. This shows that catalytic activity of Pt/C <Pt-Ni/C<Pt-Mo/C.

Figure 2,3 and 4 shows the cell performance at 318 K and that at 333 K for c. The methanol flow rate was varied from 0. 5 to 5 mL/min. The performance of the DMFC system dropped at 318 K for all flow rates in comparison with 333K. The lower flow rate showed a slightly better performance. At 333. Both the open circuit voltage and the current density decreased with increasing flow rate. Although a similar tendency was observed at 318 K, the dependence of the methanol flow rate on the DMFC performance was small because of the low temperature.

Figure 2, 3 and 4 shows the cell performance at 318 K/333K at different methanol concentrations with the flow rate of 0.5 mL to 5 mi/min. The open circuit voltage decreased with increasing the methanol concentration to 3 mol/L, because the crossover of methanol formed a mixed potential.

It ia observed from the graph that cell performance is batter at higher temperature and lower rate of anod feed.

Variation of Cell voltage With respect Tocrent density fig.5 shows the better catalytic activity of Pt-Mo/C over PT-Ni/c and Pt/C. performance of Pt-Ni/C is found to be better than Pt/c.

Addition of 50 ppm CO in the a nod flow degrades catalyst this can be shown by potential drop (Fig.5, 6, 7). In presence of CO Pt-Mo/C was found to be showing more tolerance towards CO compare to pt/C and Pt/C. The effect of addition of 50 ppm K<sub>2</sub>Cr<sub>2</sub>O<sub>7</sub> and K<sub>2</sub>CrO<sub>4</sub> in the stream of methanol and CO was not found to have positive effect on the system. It is obsreved that cell voltage further decreases on addition of K<sub>2</sub>Cr<sub>2</sub>O<sub>7</sub> and K<sub>2</sub>CrO<sub>4</sub>.

Effect of temperature on Surface process at pt(III) - H, Oxide formation and co oxidation are well studied; J phy chemB 1999, 103, 8568-8577, N.M. Markovic. T.J Schmidt & others. The chemisorption bond energy of the OH ad state is reported to be temperature dependent pt. -Ohab bond energy is reported as -136 kj/mol. Gibbs energy of adsorption ΔGHupd Θ is a function of coverage at varing temperature is given by langmuir equatron assuming 1<sup>st</sup> order kinetics as,

$$\frac{\Theta}{1-\Theta} = \exp\left(-\frac{ErheF}{RT}\right) \exp\left(-\frac{\Delta Gupd \Theta}{RT}\right) \text{-----} 1$$

The Gibbs energy of adsorption is assumed to vary linearly with coverage,

$$\Delta GHupd = \Delta GHupd \Theta = 0 + \gamma \Theta \text{-----} 2$$

Eqn 1 & 2 produces,

$$\frac{\Theta}{1-\Theta} \exp\left(\gamma \frac{\Theta}{RT}\right) = \exp\left(-\frac{ErheF}{RT}\right) * \exp\left(-\frac{\Delta Gupd \Theta}{RT}\right) \text{-----} 3$$

ΔG Hupd Θ = 0 is initial zero coverage energy of adsorption. Equation 3 produces a linear Θ v/s E relation for intermediate value of Θ, since the term Θ/(1-Θ) = 1 and verymuch more slowly with E than the exponential terms.

The apparent free energy of adsorption at any given

temperature is characterised by two parameters  $\Delta G$  and  $\Theta=0$  and interaction parameter  $f$ ;  $f = \gamma/RT$ .

The isosteric heat of adsorption can be obtained from temperature dependence of Gibbs free energy of adsorption  $q_{st}$  from the relation

$$q_{st} = \partial \left( \frac{\Delta G_{upd}}{T} \right) \frac{\partial}{\partial T^{-1}}$$

And the entropy of adsorption from the relation

$$\Delta S_{upd} = \partial \left( \frac{\Delta G_{upd}}{T} \right) \frac{\partial}{\partial T^{-1}}$$

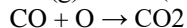
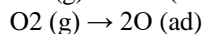
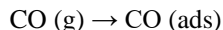
Has been reported that heat of adsorption shows linear variation with  $\Theta$  from 42 kJ/mol to 24 kJ/mol.

The Pt-OH bond energy was estimated as 350 kJ/mol.

The heat of adsorption of CO on the surface of Pt varies from 140 kJ/mol to 45 kJ/mol.

Journal of physical chemistry vol. 92.

The Langmuir-Hinshelwood reaction between adsorbed CO and O atom is well studied and given as,



From the above rate expression can be formulated as,

$$\Delta d \frac{\{CO_2\}}{dt} \rightarrow K_{exp} \left( - \frac{E_{desCO}}{RT} \right) \frac{P_{O_2}}{P_{CO}}$$

The activation energy varies from 33 to 13 k cal/mol.

Pu-238 is a radio active isotope and very powerful  $\alpha$  emitter. Plutonium-238 is a special material that emits steady heat due to its natural radioactive decay. Several unique features of plutonium-238 have made it the material of choice to help produce electrical power. Plutonium-238 has a specific power of 0.56 watts/gm. Pu in form of Plutonium oxide doped Pt-Pu/C catalyst is assumed to have maximum tolerance towards CO as Pu acts as a continuous source of thermal energy for longer period.

## References

1. Thomas S, Zalowitz M. [http:// education.lanl.gov/RESOURCES/fuelcells](http://education.lanl.gov/RESOURCES/fuelcells).
2. Perry ML, Fuller TF. J Electrochem. Soc. 2002; 149:S59.
3. Kordesch K, Simader G. Fuel Cells and Their Applications, VCH, Weinheim, 1996.
4. Hirschenhofer JH, Stauffer DB, Engleman RR, Klett MG. Fuel Cell Handbook, for USDOE, Parsons Corp., Reading, PA, 2002.
5. Blomen L, Mugerwa MN. Fuel Cell Systems, Plenum, New York. with S. Gottesfeld, with T. Zawodzinski., Polymer electrolyte fuel cells, in: C. Tobias, H. Gerischer, Kolb D., Alkire R. Eds., Advances in Electrochemistry and Electrochemical Engineering, 1993, 5:6.
6. Kordesch K, Simader G. Fuel Cells and Their Applications, VCH, Weinheim, 1996.
7. Hirschenhofer JH, Stauffer DB, Engleman RR, Klett MG. Fuel Cell Handbook, for USDOE, Parsons Corp., Reading, PA, 2002.
8. Blomen L, Mugerwa MN. Fuel Cell Systems, Plenum, New York, 1993.
9. Raistrick ID. in: RE. White, K. Konishita, J. W. Van Zee, H. S. Burney (Eds.),
10. Watanabe M, Motoo S. J Electroanal. Chem. 1975; 60:275.
11. Perry ML, Fuller TF. J Electrochem. Soc. 2002; 149:S59.
12. Bellows RJ, Marucchi-Soos EP, Buckley DT. Ind. Eng. Chem. Res. 1996; 35:1235.
13. Springer T, Zawodzinski T, Gottesfeld S. in Electrode Materials and Processes for Energy Conversion and Storage IV, J. McBreen, S. Mukerjee, S. Srinivasan, Editors, PV The Electrochemical Society. 1996; 97-13:139,
14. Carrette LP, Friedrich KA, Huber M, Stimming U. Phys. Chem. Chem. Phys. 2001; 3:320.
15. Luczak FJ, Landsman DA. US-PS 4 677 092 to International Fuel Cells, 1987.
16. Dufner BF. WO 91 / 19 566 to International Fuel Cells, 1991.
17. Buchanan JS, Hards GA, Cooper SJ. GB 2 242 203 A to Johnson Matthey PLC, 1990.
18. Zhang JX, Datta R. Electrochem. Solid-State Lett. 2003; 6:A5.